Time-lapse AVO inversion: model building and AVA analysis

A. Nassir Saeed, Laurence R. Lines, and Gary F. Margrave

ABSTRACT

Quantitative estimates of the change in reservoir properties can be accomplished by combining rock physics model along with estimated change of P- and S-impedance from time lapse seismic data. The estimated attributes are key steps in discriminating fluid saturation and pressure changes in reservoir.

In this report, we have built a time-lapse model for the Pikes Peak area. The elastic physical parameters are carefully selected based on well logs from the survey area. The synthetic P-P and P-S seismic data generated from the model, using CREWES "SYNGRAM", are being tested by proposed time-lapse inverse algorithms being developed. The AVA analysis conducted in this study produces information about rock interfaces only, and aids in calibrating physical parameters used in building of the time-lapse model. The rock modulus attributes *LambdaRho (λρ)* and *MuRho (μρ*) computed from dipole sonic log of the Pikes Peak area help in discriminating lithology, while resistivity and porosity logs give an indication about expected fluid type in the reservoir.

INTRODUCTION

AVO analysis can be considered as a direct diagnostic tool in hydrocarbon detection. In reservoir monitoring, changes in seismic attributes are often associated to the change in rock properties. Differences in reflection amplitude and other seismic attributes of the base and monitor surveys data are used in evaluating the spatial distribution of reservoir attributes and characterizations (LandrØ, 2001).

As part of an on-going research in time-lapse AVO inversion, the objectives in this report are to build time lapse model and then generating synthetic P-P and P-S seismic data for the Pikes Peak area based on available well logs and seismic data that acquired over two different times. Other goals in this study are to perform analysis for the amplitude variation with angle of the model as well as to the well logs nearby survey area.

PIKES PEAK AREA

The Pikes Peak heavy-oil field is located 40 km east of Lloydminster, border of Alberta/ Saskatchewan (Township 55, Range 23W3). Heavy oil is produced from the sands of the Waseca Formation (figure 1) of the Lower Cretaceous Mannville Group (Watson, 2004). The Pikes Peak field itself is located on an east-west structural high within an incised valley-fill channel complex (Sheppard et al.,

1998). Based on well logs from that field, the Waseca Formation lies at depth of about 475-510 m and has an average thickness of 15-25 m.

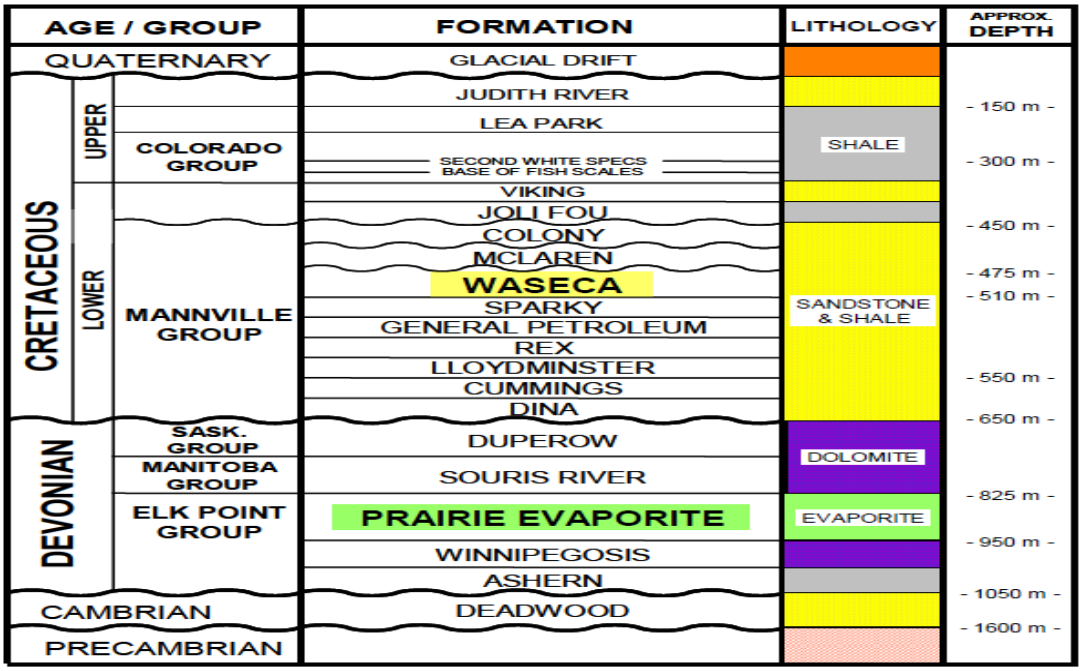

FIG.1 Stratigraphic chart for the Pikes Peak area (*after Core laboratories; Watson, 2004*).

WELL LOGS ANALYSIS

Two well logs that are closely located to the time lapse seismic survey lines (figure 2) are used in this study. Figure (3) shows different logs for the well 15A-6 that was drilled and logged in February, 2000. Notice the substantial change in P-wave velocity compared to the S-wave velocity at Waseca reservoir zone.

Several seismic rock properties are computed from dipole sonic of well 15A-6, of Pikes Peak area. Note that for subsequent scattering graphs, data points are colored by Gamma rays. Furthermore, estimated seismic rock properties for the upper Quaternary, Viking, and Waseca formations are colored in solid green, black and magenta respectively.

Figures (4-6) show different displays of the seismic rock parameters that aid in lithology discriminations. The Viking formation in figure (4) shows high values of shear modules, while the Waseca formation shows fair shear and Lamé values. In figure (5), the Viking formation shows distinct low Mu and Lamé values compared to the Waseca formation. In Figure (6) the Quaternary formations shows high Poisson ratio and lower P-wave, compared to the Viking formation.

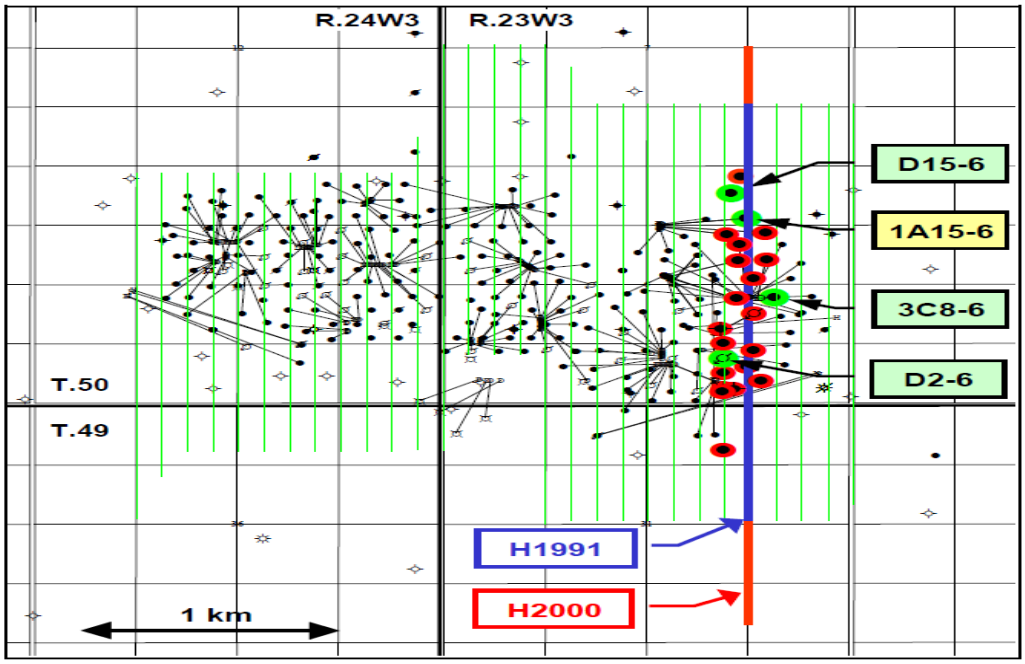

FIG.2 Map of the Pikes Peak area shows locations of well logs, injection and production wells along with time-lapse seismic survey lines (*after Watson, 2004*).

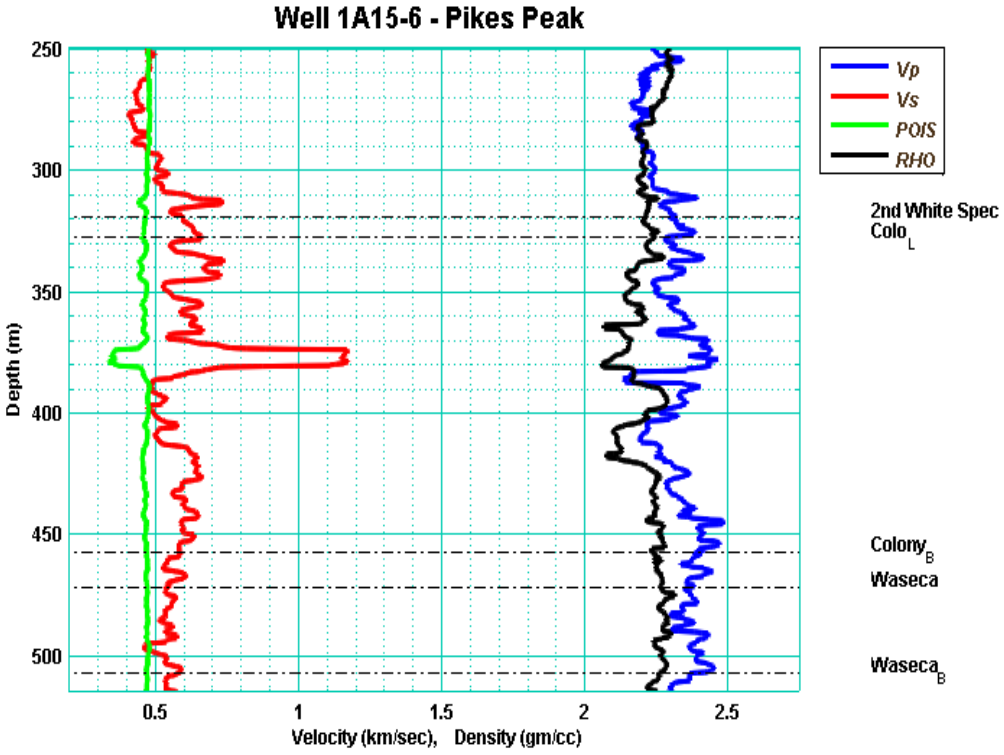

FIG.3. Well 15A-6, Pikes Peak field shows Vp, Vs, Poisson and density logs.

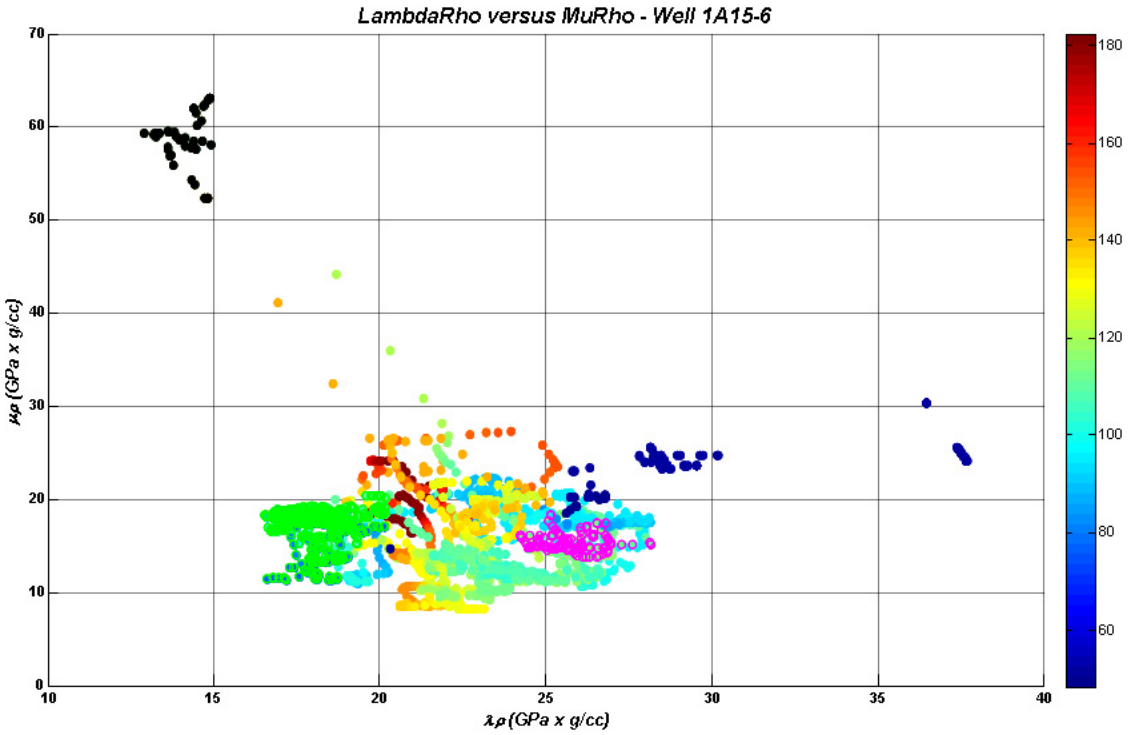

FIG.4 *LaméRho* versus *MuRho* for Well 15A-6, Pikes Peak field.

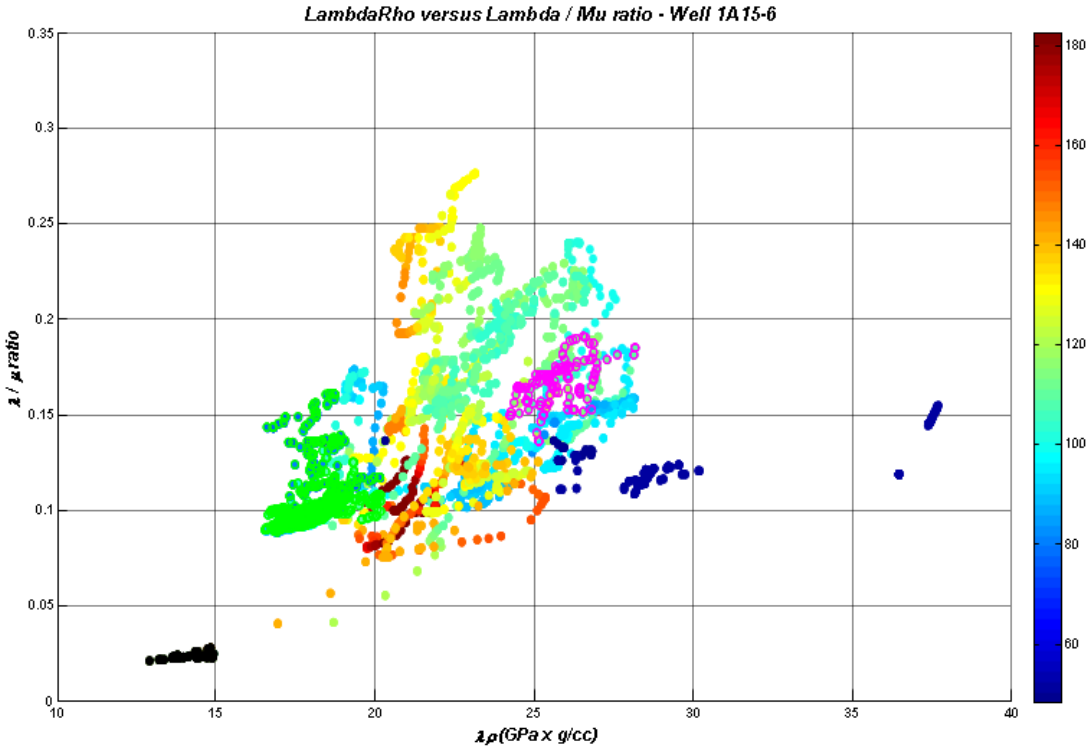

FIG.5 *LaméRho* versus *Lamé / Mu* for Well 15A-6, Pikes Peak field.

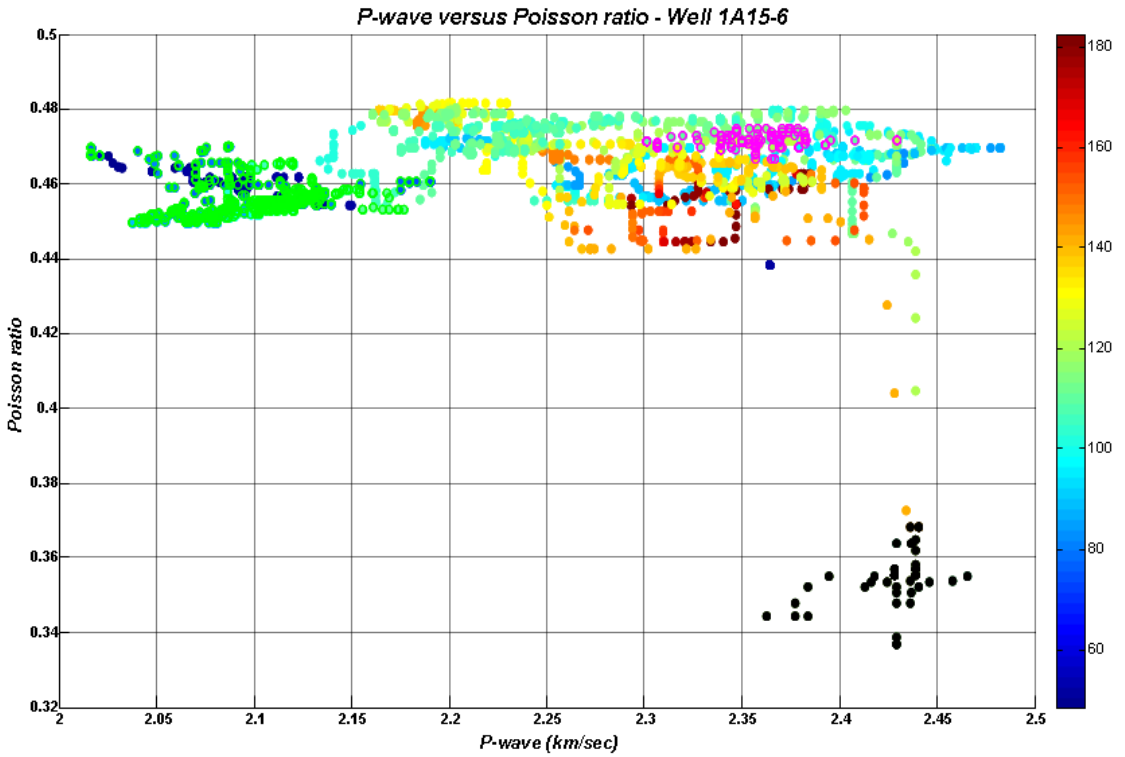

FIG.6 P-wave velocity versus Poisson's ratio for Well 15A-6, Pikes Peak field.

The resistivity logs of well D2-6 (figure 7), which was logged in year 1980 shows high values for Waseca oil reservoir, while figure (8) depicts the neutron- and density-porosity logs. Note that the cross-over of neutron and density indicates the presence of gas.

In summary, well logs from Pikes Peak area shows distinctive changes in physical measured values for the Waseca heavy oil reservoir zone that will aid in defining zone of interest in building time-lapse model.

TIME-LAPSE MODEL BUILDING

For the Pikes Peak oil field, Zou et al., (2006), have shown a build-up in the amplitude of the migrated seismic section of line H2000 compared to the migrated section of H1990 seismic line. Amplitude build-up in the seismic migrated section can be attributed to the gas accumulating due to the cyclic steam stimulation (CSS) process used by Husky Energy for extracting the heavy oil. When the heavy oil is heated during the CSS process, it draws the gas out of oil-phase. The reservoir simulation work by Zou, et al., (2006) indicates that seismic response is significantly affected by the gas exsolved from the oil phase. The gas saturation increases at the top of reservoir, and this confirmed by the cross-over of neutron and porosity logs in figure (8).

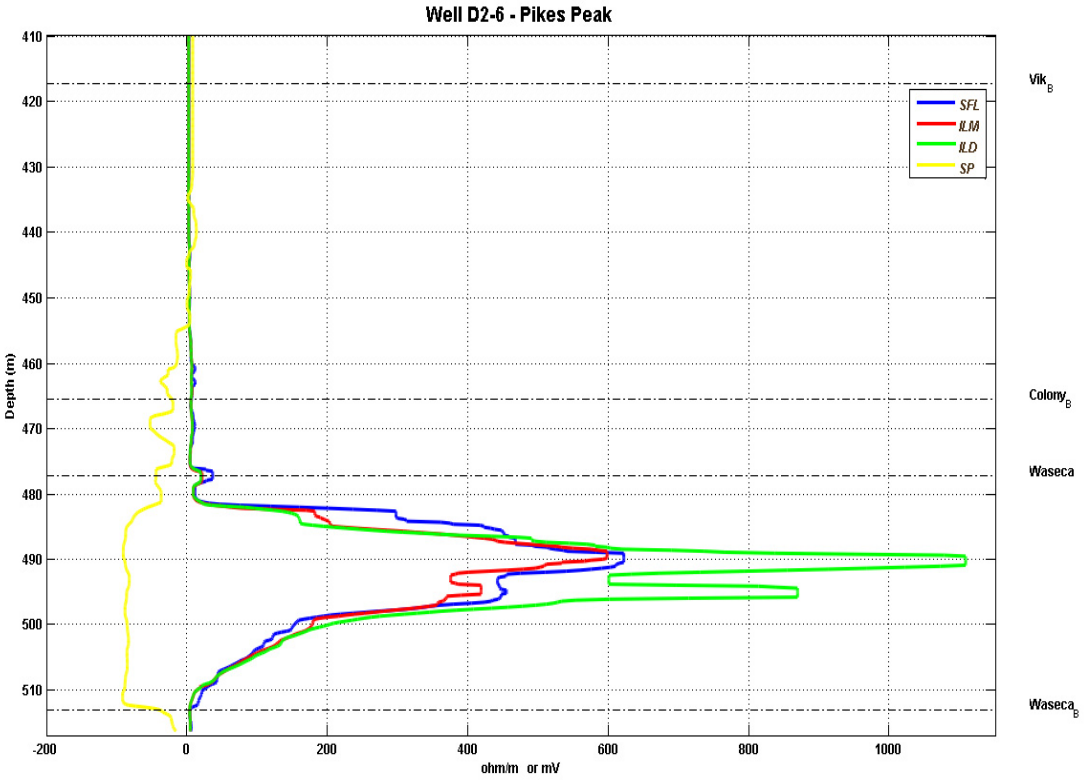

FIG.7. Resistivity and SP logs for Well D2-6, Pikes Peak field.

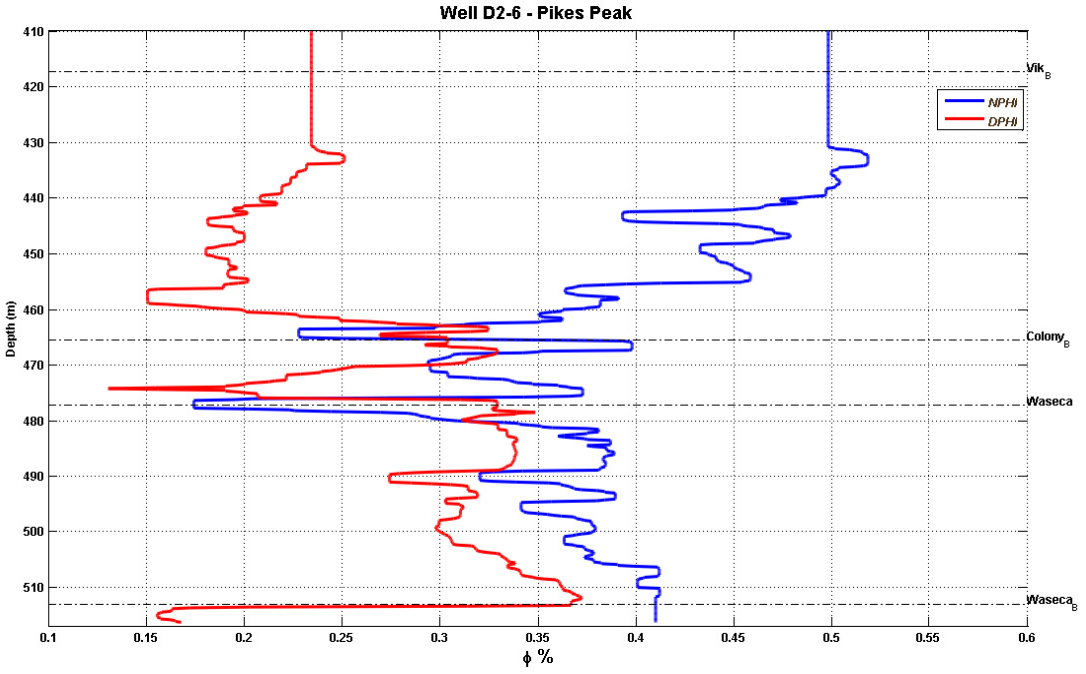

FIG.8. Neutron- and density- porosity logs for Well D2-6, Pikes Peak field. Note the cross-over between the two logs at the top of reservoir

AVO modeling is a practical aspect in seismic acquisition design, processing and interpretation of pre-stack seismic data (Li. et al., 2007). In this study, many assumptions are made in building up the time-lapse model. The model consists of three layers, where the second layer represents the reservoir. We assume that the Waseca reservoir is made up of horizontal homogenous sand interval. The elastic physical parameters (P-wave velocity, S-wave velocity and density) for the top and bottom layers were held constant for the base and two monitoring surveys, while elastic physical attributes of the middle layer were allowed to be varies over three different periods of time.

The P-wave velocity, S-wave velocity, and density values of the top layer are 3500 m/sec, 1750 m/sec and 2700 Kg/m^3 respectively, while for the bottom layer, these physical attributes were set to be 4000 m/sec, 2250 m/sec and 2900 Kg/m^3 respectively.

For the base survey, The P-wave velocity, S-wave velocity, and density values of the reservoir (middle) layer were set to be 3000 m/sec, 1500 m/sec and 2650 Kg/m^3 respectively, while for the first monitoring model, these attributes were set at 2500 m/sec, 1450 m/sec and 2500 Kg/m^3. For the second monitoring survey model, the P-wave velocity was 2000m/sec, S-wave velocity was set at 1400 m/sec while density value was 2300 Kg/m^3.

Note that we maintain constant rate of 500 m/sec for the change in P-wave velocity over lapsed time, while S-wave velocity and density values were changed at small rates compared to the P-wave velocity. This is because P-wave velocity is significantly reduced by steam injection due to CSS process. The assumption of P-wave rate of change is in consistent with previous conclusion work by Watson and Lines, (2001) for the same survey area, where the Vp/Vs ratio was noticed to be decreased at high rate over two lapse times.

Figure (9) shows the time-lapse model. The thickness of reservoir layer is slightly exaggerated in order to avoid tuning effects on seismic resolution and AVO responses (Downton, 2005). The bottom layer was terminated at a depth of 850m where Pre-camberian unconformity manifests (Watson 2004). The far offset of the model is set to be 1200m, and geophone interval at 20m so as to simulate seismic surveys that were carried out for the H1990 and H2000 survey lines. Figure (10) shows synthetic logs that generated for the time-lapse model given in figure (9).

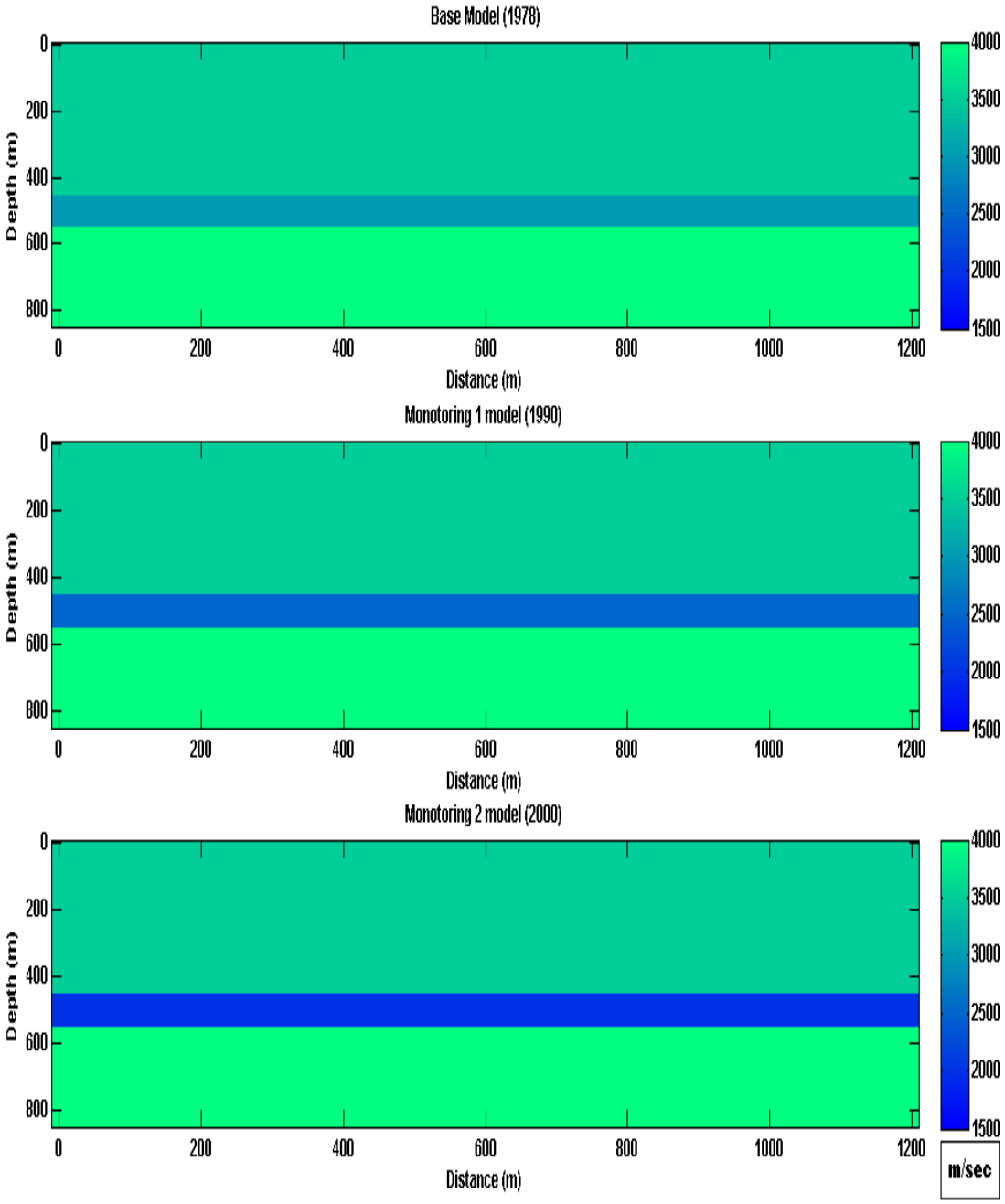

FIG.9. Time-lapse model for the Pikes Peak area. Note the change in the intensity blue color of the middle layer over time-lapse models

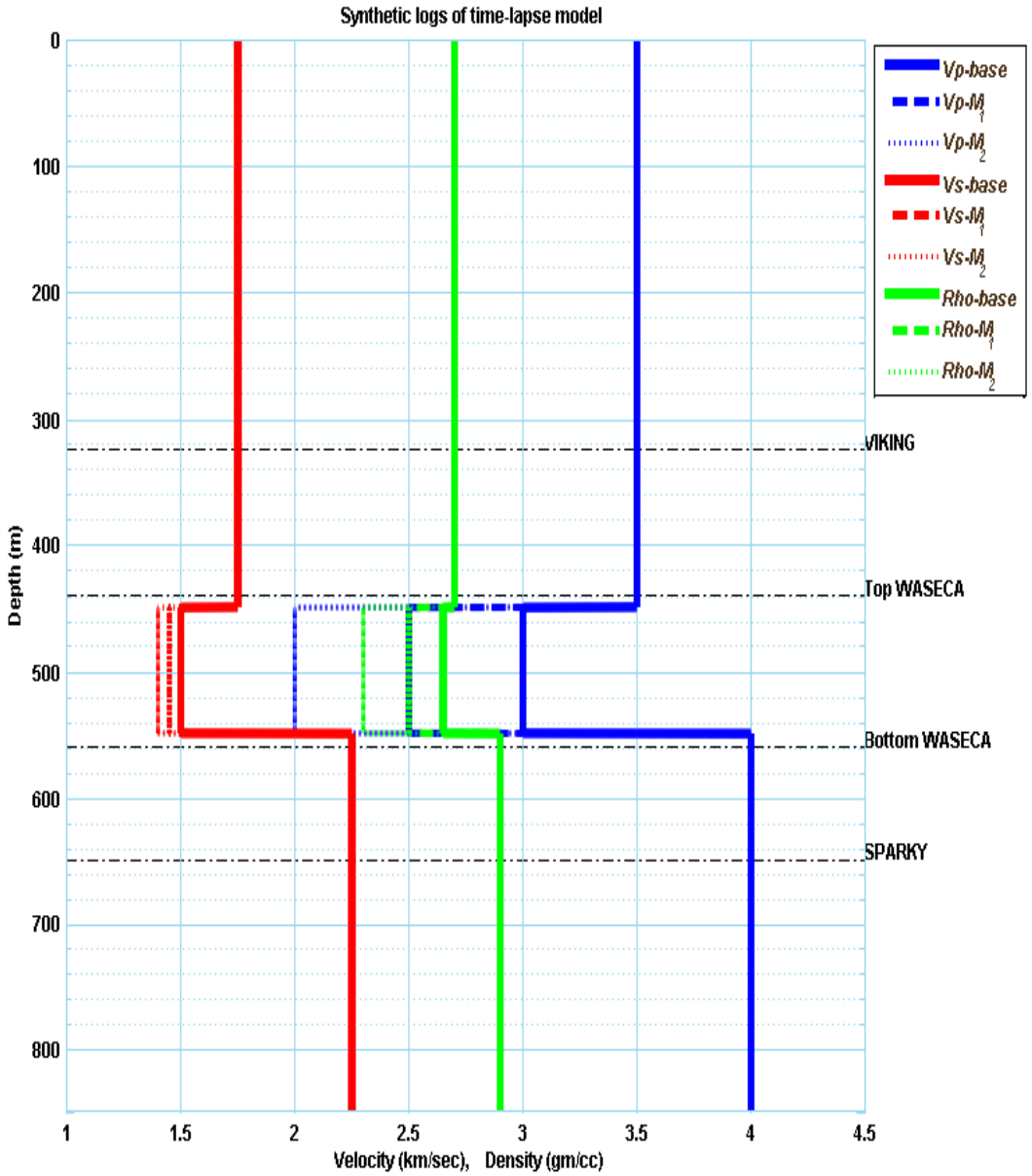

FIG.10. Synthetic logs for the time-lapse model of the Pikes Peak area.

The synthetic logs generated in this study are then used in combination with Zoeppritz equation to create P-P and P-S synthetic gathers using CREWES "SYNGRAM" tools. A Ricker wavelet of a dominate frequency of 60Hz is used for base and monitoring models assuming that source wavelets did not change during these surveys. This assumption is made in order to restrict uncertainties in estimating model parameters during time-lapse AVO inversion.

SYNTHETIC DATA

The synthetic P-P and P-S data were generated using a multi-offset synthetic seismogram, SYNGRAM, (Lawton and Howell, 1992; Margrave and Foltinek, 1995). The Vp, Vs and density models are ray-traced for PP and P-S incidence angles, and amplitudes were calculated using the Zoeppritz equations. The resulting P-P and P-S offset gathers for the base survey model are showing in figure (11), while for monitoring (1) survey are displayed in figure (12), and for monitoring (2) survey are given in figure (13). Note that the contrasts increasing and amplitude build-up of resulting sections, as we proceed from the base to the monitoring (2) survey. Also notice, the critical refraction appears after 1000m offset in the P-S synthetic gathers.

In previous section, the magnitude of S-wave and density were set to be decreasing at small rate compared to the P-wave velocity. In theory, the shear wave velocity is inversely proportional to density based on $V_s = \sqrt{\mu/\rho}$. However, in order to investigate this assumption, we have let the density of the second layer of the base model intact and let the density gradually increases as we move from monitoring (1) model towards the monitoring (2) model (i.e., we swapped the density values of monitoring surveys from original setting).

Figures (14 and15) shows the P-S synthetic sections for monitoring (1 and 2) models. Note that the amplitude contrast in both sections is decreasing as density increases. The resulting sections are in conflict with migrated sections of Zou et al., (2006). Furthermore, injecting steam during CSS process reduces the viscosity of the heavy oil, thus decreases the density. This CSS process will lead into an increase in the gas accumulation due to exsolving gas from oil-phase, and subsequently affecting seismic amplitude responses. Therefore, we concluded that density values of the reservoir layer of the time-lapse model are assumed to be decreasing with time due to steam injection.

AVA REFLECTIVITY ANALYSIS

Synthetic well log data generated in this study are then used in combination with Zoeppritz equations to numerically model the changes in P-P and P-S reflectivity with incidence angle for the time-lapse model of the Waseca formation. We performed the reflectivity analysis only for the top and reservoir layers, where the interface is a shale/sand.

Figure (16) shows that the P-P reflectivity is steadily increasing with angle until it reach maximum values, where critical angles become visible for all models curves, and then the amplitudes dive towards the end of the curves. Note that there is no change in terms of amplitude polarities for all the base and monitoring

surveys, however, it has been noticed that the magnitude of critical angle is changing from (Ø=41) for the base model to (Ø=37) for monitoring (2) model.

In figure (17), the amplitudes of P-S reflectivity for the base and monitoring models are showing reverse scenario to the P-P reflectivity. The magnitude of P-S reflection amplitude are increasing but at small magnitude compared to the P-P reflectivity, and critical angle are appearing at late angle range as we proceed from the base model (Ø=40) to a critical angle (Ø=45) for the monitoring (2) model. Note that the increase in amplitudes as angle of incidence increases is in consistent with synthetic P-S data shown in figures (11b, 12b and 13b) respectively.

CONCLUSIONS

The rock modulus attributes *LambdaRho* ($\lambda\rho$) and *MuRho* ($\mu\rho$) computed from dipole sonic log of the Pikes Peak oil field help in discriminating lithology while neutron and porosity log indicates the presence of gas. The resistivity and self-potential logs give an indication about type of fluid expected in the reservoir.

The amplitude versus angle produces information about rock interfaces only, and aids in deciding the volume of synthetic data to be used in seismic inversion. The AVA analysis does not experience polarity reversal for a given angle range of time-lapse model.

FUTURE WORK

Computer algorithms for AVO inversion of time-lapse data are being developed. New proposed inversion schemes are introduced and being tested using generated synthetic P-P and P-S data for the time-lapse model presented in this study. The successful incorporations of different constrains in the data and model spaces used for inverting of density log (Saeed et. al., 2010a and 2010b) in previous studies, give motivation to examine the stability and accuracy of the proposed time-lapse AVO inverse schemes. Also to see if improvements can be made for the estimated model parameters, in particular the reflectivity density attribute (Larsen, 1999). The accuracy of building the time-lapse model for the Pike Peak will be further investigated using Biot-Gassmann fluid substitution (Russell et al., 2003).

A)

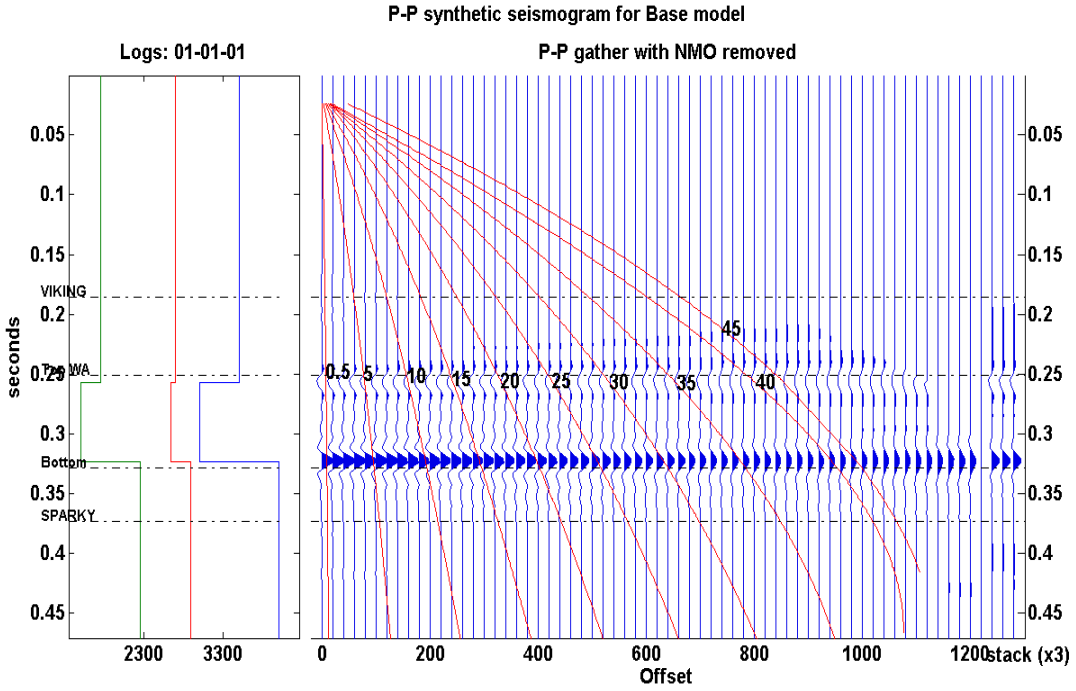

B)

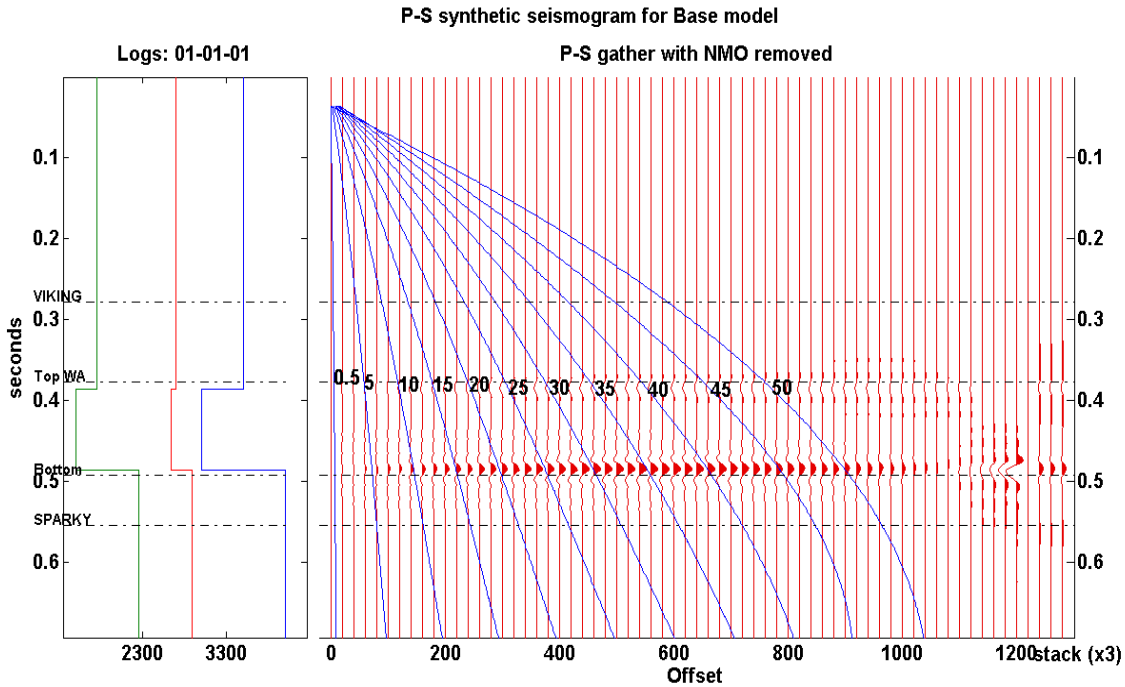

FIG.11. Synthetic seismic gathers for the base model of the Pikes Peak area. A) P-P synthetic gather. B) P-S synthetic gather.

A)

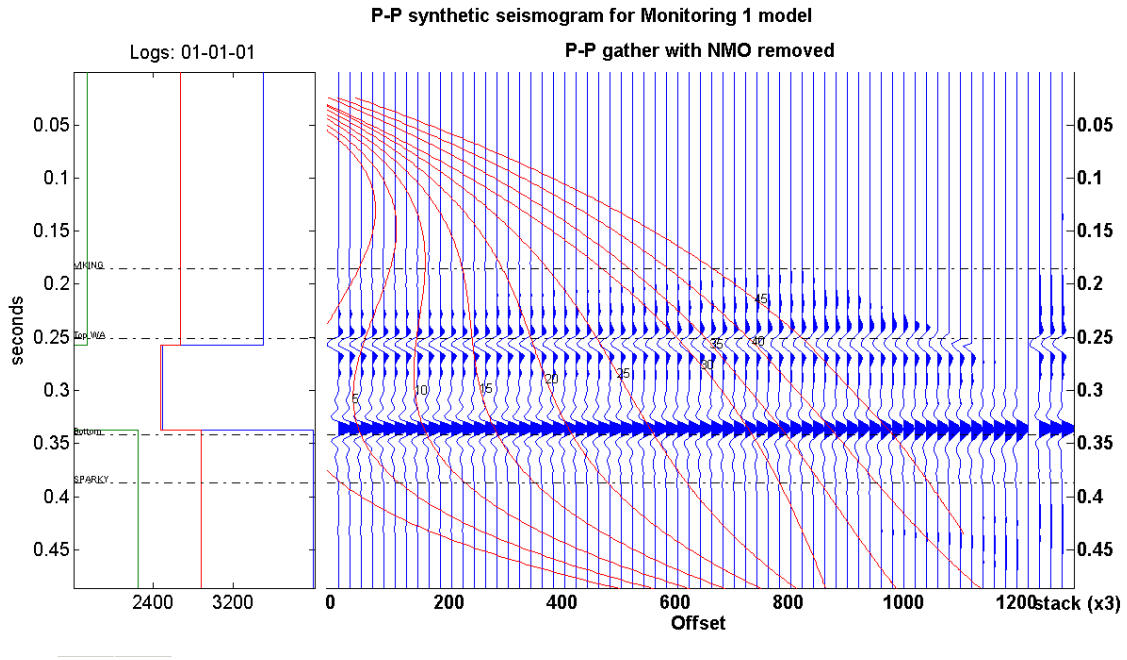

B)

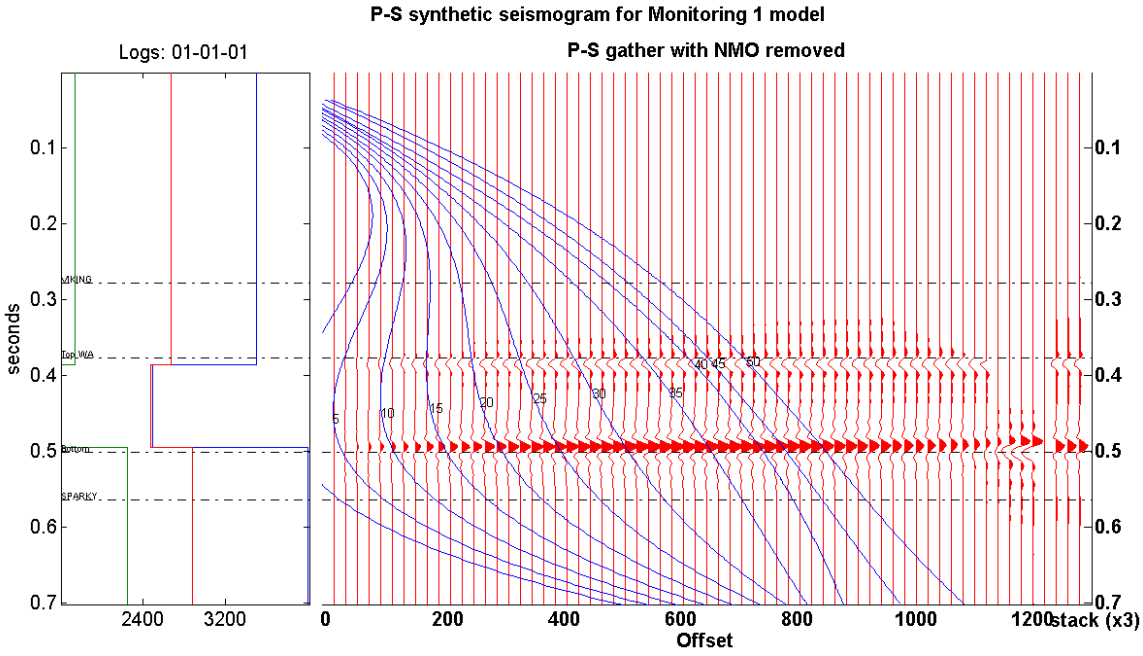

FIG.12. Synthetic seismic gathers for the monitoring (1) model of the Pikes Peak area. A) P-P synthetic gather. B) P-S synthetic gather.

A)

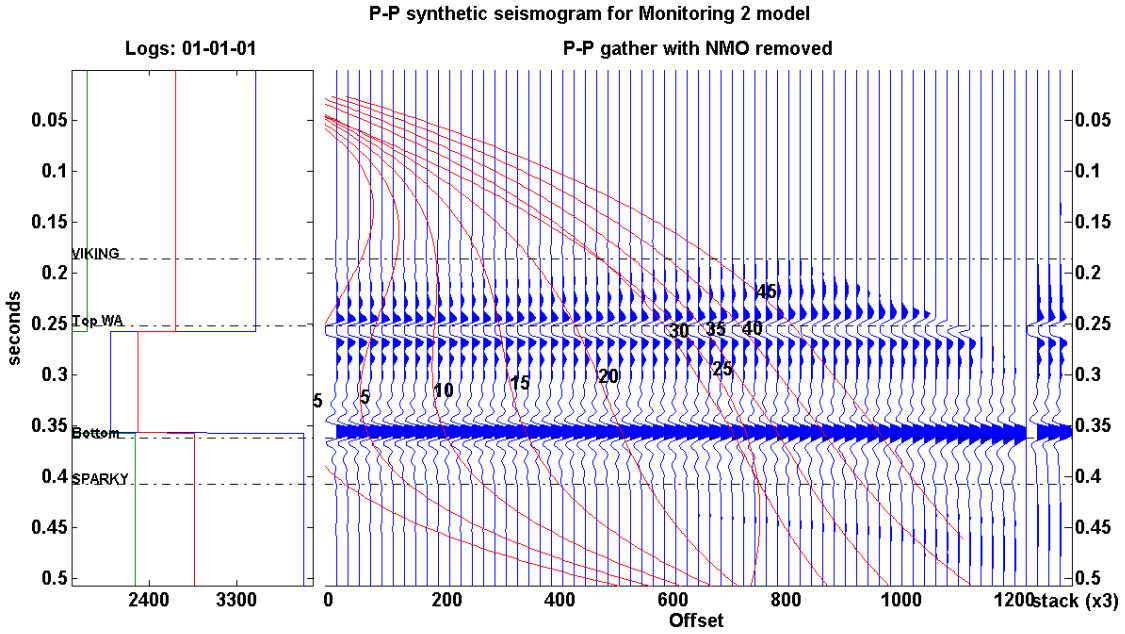

B)

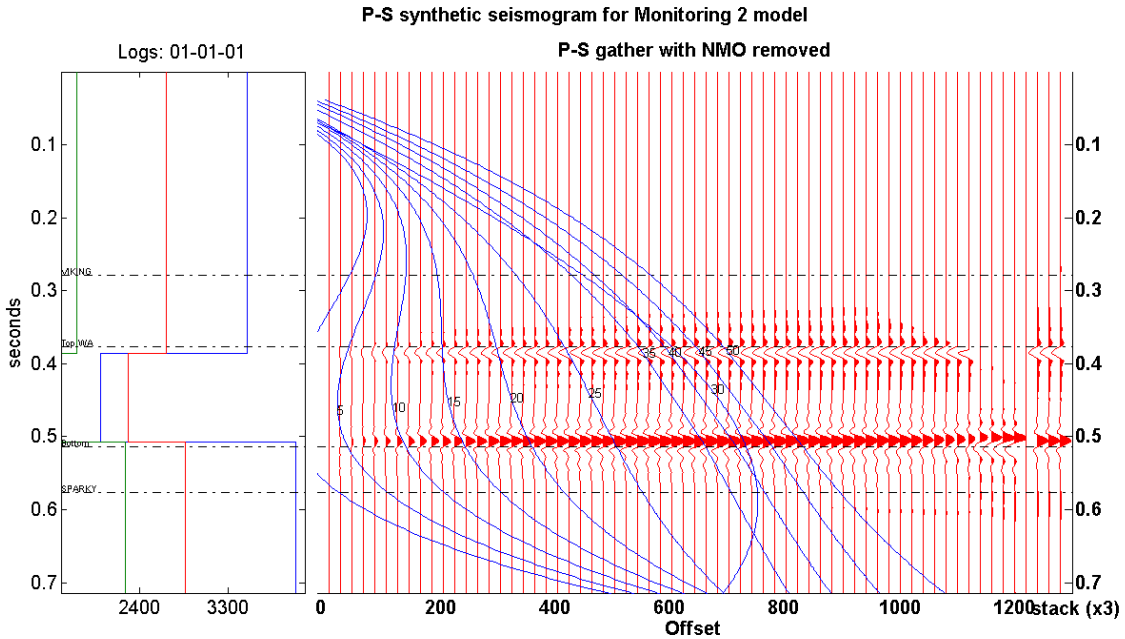

FIG.13. Synthetic seismic gathers for the monitoring (2) model of the Pikes Peak area. A) P-P synthetic gather. B) P-S synthetic gather.

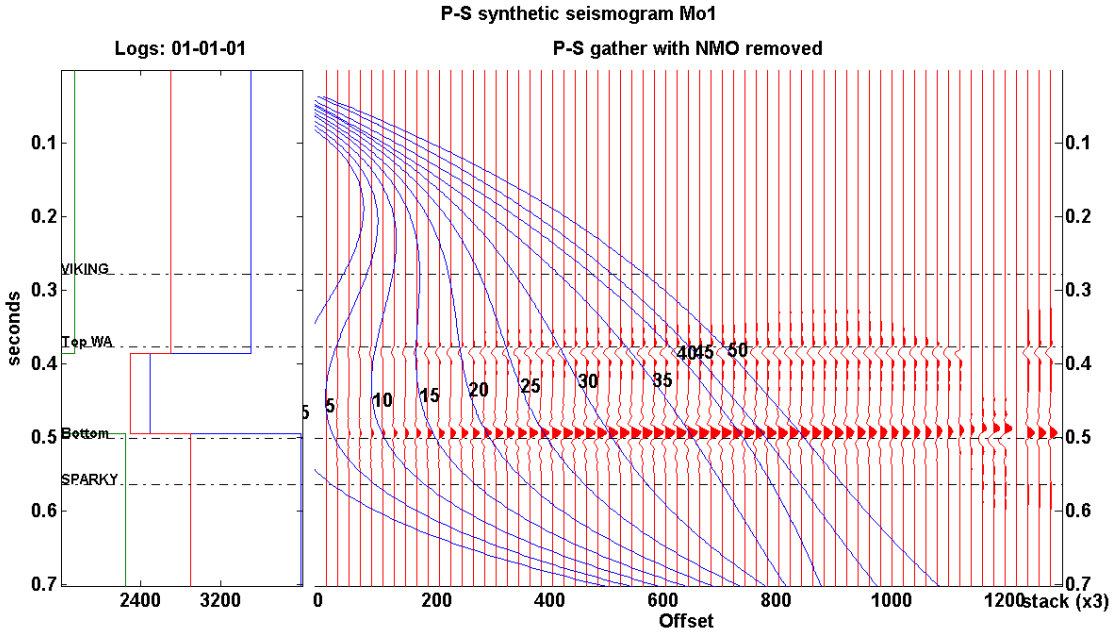

FIG.14. Synthetic P-S seismic gathers for the monitoring (1) model of the Pikes Peak area. Density values were set to be increased in magnitude from the base model.

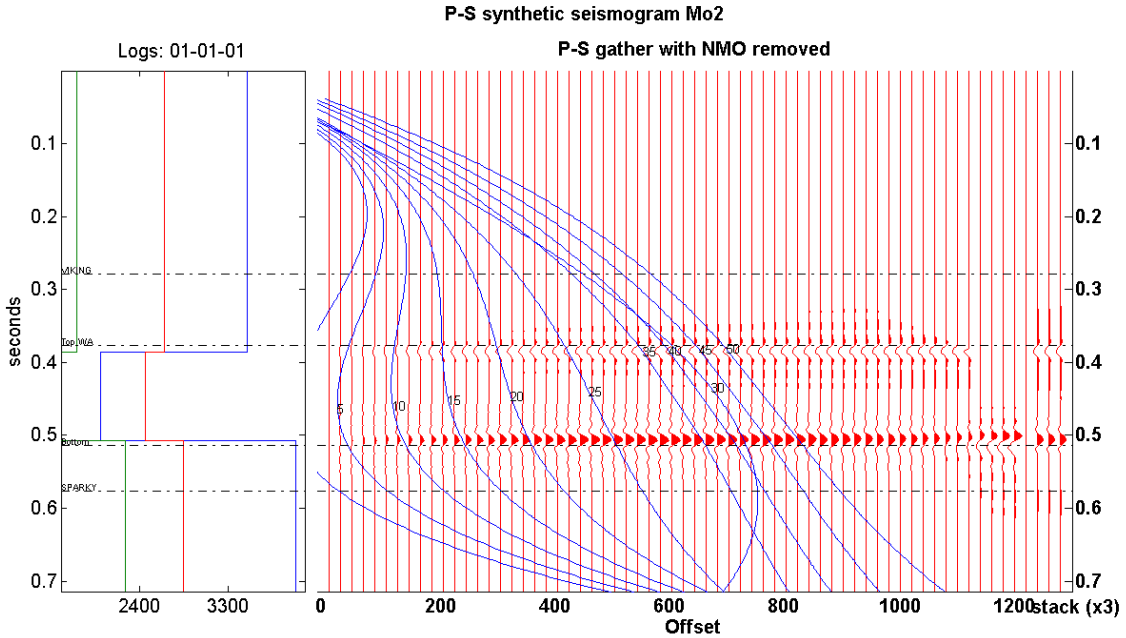

FIG.15. Synthetic P-S seismic gathers for the monitoring (2) model of the Pikes Peak area. Density values were set to be increased in magnitude from the monitoring (1) model.

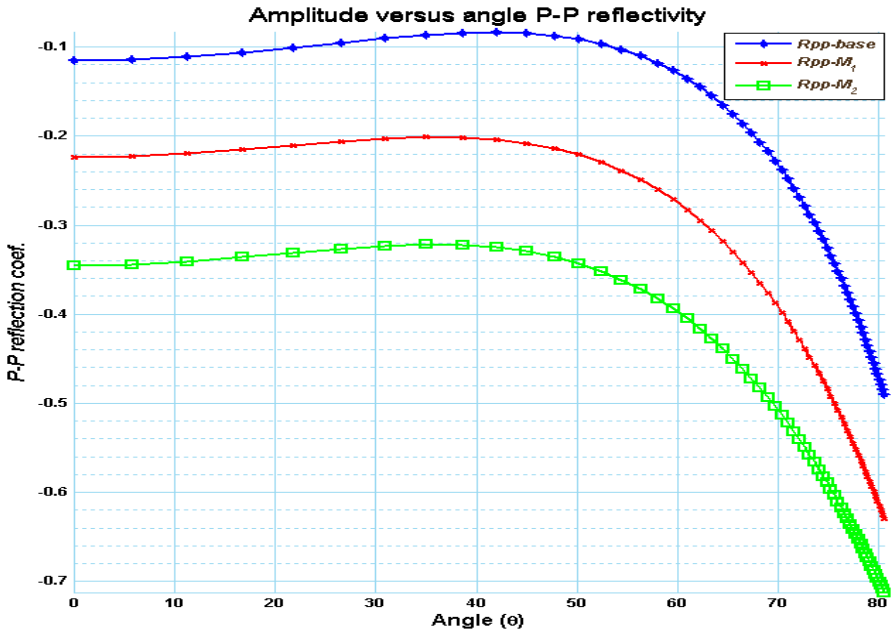

FIG.16. AVA analysis for **P-P** reflectivity of the top and reservoir layers of time-lapse model of the Pikes Peak area.

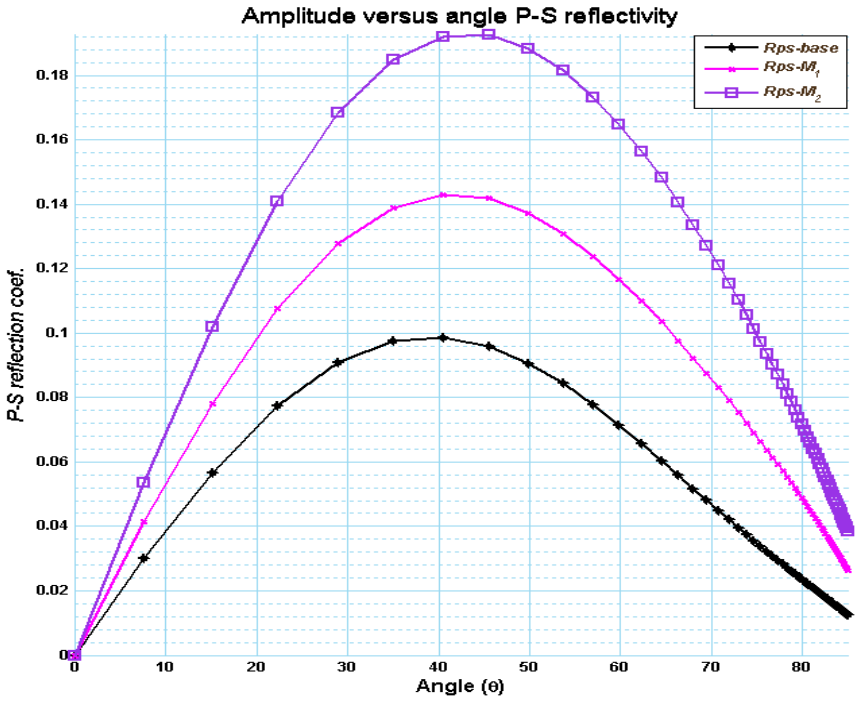

FIG.17. AVA analysis for **P-S** reflectivity of the top and reservoir layers of time-lapse model of the Pikes Peak area.

ACKNOWLEDGEMENTS

Authors would like to thank Ken Hedlin of Husky Energy for providing well logs used in this study, and all of the CREWES sponsors.

REFERENCES

Downton, J.E., 2005, Seismic parameter estimation from AVO inversion: Ph.D. thesis, university of Calgary.

LandrØ, M., 2001, Discrimination between pressure and fluid saturation changes from time-lapse seismic data: Geophysics, 66, 836-844.

Larsen, J.A., 1999, AVO Inversion by Simultaneous P-P and P-S Inversion: MS.c. thesis, university of Calgary.

Lawton, D.C., and Howell, T.C., 1992, P-P and P-SV synthetic stacks, Expanded Abstract, 62nd SEG Ann. Internat. Mtg., 1344-1347.

Li, Y., Downton, J.E., and Xu, Y., 2007, Practical aspects of AVO modeling: The leading Edge, **26**, 295-311.

Margrave, G.F., and Foltinek D.F., 1995, Synthetic P-P and P-SV cross sections: CREWES report, **7**.

Russell, B., Hedlin B., Hilterman, F., and Lines, L., 2003, Fluid-property discrimination with AVO: A Biot-Gassmann perspective: Geophysics, **68**, 29-39.

Saeed, A.N., Lines, L.R., and Margrave, G.F., 2010a, Iteratively re-weighted least squares inversion for the estimation of density from well logs: part one: CREWES report, **22**.

Saeed, A.N., Lines, L.R., and Margrave, G.F., 2010b, Iteratively re-weighted least squares inversion for the estimation of density from well logs: part two: CREWES report, **22**.

Sheppard, G.L., Wong, F.Y. and Love, D., 1998, Husky's success at the Pikes Peak Thermal Project: Unitar Conference, Beijing, China, Expanded Abstracts.

Watson, I.A., 2004, Integrated geological and geophysical analysis of a heavy-oil reservoir at Pikes Peak, Saskatchewan: MS.c. thesis, university of Calgary.

Watson, I.A. and Lines, L.R., 2001, Time-lapse seismic monitoring at Pikes Peak, Saskatchewan: 2001 CSEG Annual Mtg, Calgary, Alberta.

Zou, Y., Bentley, L.R., and Lines, L.R, D., 2006, Integration of seismic methods with reservoir simulation, Pikes Peak heavy-oil field, Saskatchewan: The leading Edge, **25**, 764-781.